CrystEngComm

ROYAL SOCIETY OF CHEMISTRY

PAPER

View Article Online
View Journal | View Issue

Cite this: *CrystEngComm*, 2025, **27**, 1292

Surfactant-free co-solvent exfoliation strategy for semiconducting quasi-1D $Nb_2Pd_3Se_8$ nanowires†

Kyung Hwan Choi,‡[b] Yeongjin Kim,‡[a] Jinsu Kang,[a] Kyung In Kim,[a] Jeong Su Park,[a] Hyung-Suk Oh,[ade] Hak Ki Yu *[c] and Jae-Young Choi *[abe]

Received 8th November 2024,
Accepted 9th January 2025

DOI: 10.1039/d4ce01136h

rsc.li/crystengcomm

$Nb_2Pd_3Se_8$, a quasi-one-dimensional (1D) van der Waals material, has recently gained attention owing to its intriguing structural, electrical and optoelectrical properties. In this work, we studied co-solvent exfoliation of $Nb_2Pd_3Se_8$ in a mixture of water and ethanol or isopropanol. By adjusting the compositions of the co-solvent, the dispersion behavior of $Nb_2Pd_3Se_8$ was interpreted in terms of surface tension and dielectric constant. This approach is effective for substituting the previously reported optimal solvent of NMP, which is toxic with a high boiling point of 204 °C. The $Nb_2Pd_3Se_8$ nanowire prepared through co-solvent exfoliation presented a high electronic property with an electron mobility of 10.3 $cm^2 V^{-1} s^{-1}$.

1. Introduction

One-dimensional (1D) van der Waals (vdW) materials have recently attracted attention because of their unique structural, physical, electrical and magnetic properties.[1–4] In particular, the ultimate downscaled structure, known as a 1D single-chain atomic crystal, holds promise for the fabrication of highly integrated electronic devices owing to its minimized dimensionality and lack of dangling bonds on surfaces.[5–7] Extensive research has been conducted on these materials to address the stability at the ultimate atomic scale and explore associated downscaling processes.[8–11]

Recently, we successfully prepared a novel quasi-1D vdW $Nb_2Pd_3Se_8$ material as a promising semiconducting building block for nano-electronic fields.[12–14] Its dissociative nature allowed for the separation of several nanometers thick $Nb_2Pd_3Se_8$ nanowires *via* mechanical exfoliation technique. The properties of mechanically exfoliated $Nb_2Pd_3Se_8$ nanowires have been intensively studied for application in field-effect transistors (FETs) and photodetectors.[12,15] Furthermore, research on liquid phase exfoliation of $Nb_2Pd_3Se_8$ has been studied to expand the preparation methods.[16] By testing various exfoliation solvents, it was confirmed that *N*-methyl-2-pyrrolidone (NMP) is the optimal solvent for exfoliation and stabilization of $Nb_2Pd_3Se_8$ nanowires owing to its well-matched surface tension and polarity. However, NMP is considered highly toxic, and its high boiling point of 204 °C limits its broader applications.[17]

In this work, we utilized a co-solvent exfoliation strategy using a mixture of water and ethanol (EtOH) or isopropanol (IPA) to identify alternative exfoliation solvents without using a dispersant (Scheme 1). We tested a total of nine solvent compositions for each co-solvent system to compare the dispersibility of $Nb_2Pd_3Se_8$.

2. Experimental section

2.1 Synthesis of $Nb_2Pd_3Se_8$

$Nb_2Pd_3Se_8$ was prepared using Nb powder (99.99%, Alfa Aesar), Pd powder (≥99.9, Alfa Aesar) and Se powder (99+%, Alfa Aesar). A stoichiometric mixture of Nb, Pd and Se was pelletized and sealed in a 10 cm-long evacuated quartz tube. The sealed quartz tube was placed inside a box furnace and heated at 600 °C for 120 h before cooling at 4 °C h^{-1}. The resulting material was a dark grey sintered powder.

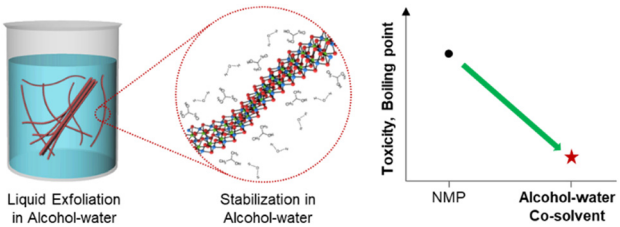

Scheme 1 Co-solvent exfoliation strategy of $Nb_2Pd_3Se_8$ nanowires for substituting the conventional, highly toxic, high-boiling point NMP solvent.

[a] *School of Advanced Materials Science & Engineering, Sungkyunkwan University, Suwon, 16419, Korea. E-mail: jy.choi@skku.edu*
[b] *SKKU Advanced Institute of Nanotechnology (SAINT), Sungkyunkwan University, Suwon, 16419, Korea*
[c] *Dept. of Materials Science and Engineering & Dept. of Energy Systems Research, Ajou University, Suwon, 16499, Korea. E-mail: hakkiyu@ajou.ac.kr*
[d] *Clean Energy Research Center, Korea Institute of Science and Technology, Seoul, 02792, Korea*
[e] *KIST-SKKU Carbon-Neutral Center, Sungkyunkwan University, Suwon, 16419, Korea*

† Electronic supplementary information (ESI) available. See DOI: https://doi.org/10.1039/d4ce01136h

‡ These authors contributed equally to this work.

2.2 Liquid phase exfoliation

Initially, 10 mg of $Nb_2Pd_3Se_8$ powder was immersed in 10 mL of each solvent. The initial large powder particles were crushed *via* ultrasonication using a probe sonicator (VC 505, Sonics & Materials, Inc.). The probe sonicator was operated for 5 min at a 2 s on/2 s off interval. Subsequently, bath sonication (B2005S-68 K, 68 kHz, 200 W, KODO Technical) was conducted for 3 h. After ultrasonication, centrifugation at 6000 rpm for 10 min was performed to remove insufficiently dispersed chains.

2.3 Characterization

X-ray diffraction (XRD, D8 Advance, Bruker) was performed using Cu-Kα radiation (λ = 0.154 nm) at a scan rate of 5° min^{-1}. Morphological and compositional analyses were conducted using field-emission scanning electron microscopy (FE-SEM, Hitachi, S-4300SE). Topographic analysis was performed in a tapping mode using a Park system with Si cantilevers (~300 kHz resonant frequency) coated with Al (Tap300 Al, Budget Sensors Inc.) with a scan rate of ≈0.4 Hz. UV-visible absorbance was determined using a UV-vis spectrophotometer (Agilent Technologies Inc., Agilent 89090A).

2.4 Device fabrication

$Nb_2Pd_3Se_8$ nanowires exfoliated in 50% IPA were chosen for device fabrication. $Nb_2Pd_3Se_8$ dispersion was spin-coated on a highly doped SiO_2 (100 nm)/Si substrate. The device was patterned using the standard photolithography method, and the Cr/Au (5/50 nm) electrodes were deposited using an e-beam evaporator under high vacuum conditions.

3. Results and discussion

$Nb_2Pd_3Se_8$ consists of the smallest unit ribbon structures forming in a zigzag shape (Fig. 1a). As studied in a previous report, the inter-ribbon forces exhibit a low binding energy as weak as that exhibited by vdW forces, allowing miniaturization through the exfoliation process.[12] Bulk $Nb_2Pd_3Se_8$ powder was synthesized through the solid-state reaction of elements at 600 °C, as described in previous studies.[16] As shown in the SEM image, the bulk crystals are of several micrometers in size and consist of separable wire-like structures (Fig. 1b). The obtained powder was further characterized using X-ray diffraction and Raman spectroscopy, resulting in the well-matched diffraction pattern and vibration modes, respectively (Fig. 1c and d).

Co-solvent exfoliation of $Nb_2Pd_3Se_8$ was performed using nine different mixing volume ratios with varying alcohol content (Table 1). $Nb_2Pd_3Se_8$ powder was immersed in each solvent with an initial concentration of 1 mg mL^{-1}. Next, the starting solutions were ultrasonicated and centrifuged at 6000 rpm to obtain the resulting dispersions. Fig. 2a and b show images of the representative final $Nb_2Pd_3Se_8$ dispersions processed in EtOH–water and IPA–water. When

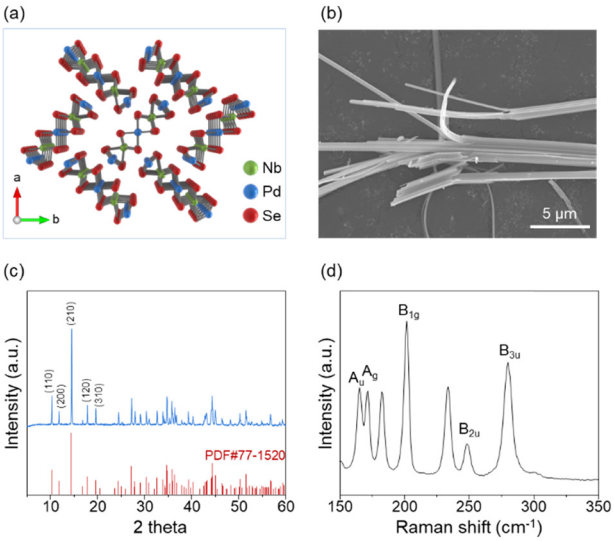

Fig. 1 (a) Crystal structure of orthorhombic $Nb_2Pd_3Se_8$ (Pbam). (b) SEM image of the bulk $Nb_2Pd_3Se_8$ crystals. (c) XRD pattern of the bulk $Nb_2Pd_3Se_8$ crystals. (d) Raman spectrum of $Nb_2Pd_3Se_8$ measured under an excitation wavelength of 785 nm.

using water (0%) and ethanol (100%) as single solvents, successful exfoliation of $Nb_2Pd_3Se_8$ was not observed. However, in the case of co-solvent, dark-colored dispersions were produced, indicating effective exfoliation. In the case of IPA–water, sufficient exfoliation was observed over a wider range of volume ratios compared to EtOH–water. The images for all solvent compositions are summarized in Fig. S1.† To compare the concentration of $Nb_2Pd_3Se_8$ nanowires in each solvent, UV-visible absorbance was performed for all test solvents (Fig. S2 and S3†). The concentrations of the dispersions were evaluated based on the measured absorbance at a wavelength of 400 nm (Fig. 2c). Overall, the IPA–water system revealed higher dispersibility than EtOH–water. To investigate the dispersion behavior of $Nb_2Pd_3Se_8$, the absorbance results were plotted as a function of the surface tension of solvents used (Fig. 2d). First, as described earlier, there was no exfoliation in water (72.75 mJ m^{-2}). Then, as EtOH or IPA was introduced into the solvent system, a peak in the exfoliation yield started to appear. Notably, an upturn in the absorbance curve was observed for EtOH–water at 30% (35.0 mJ m^{-2}), whereas IPA–water showed high exfoliation yield even at 20% (33.87 mJ m^{-2}), indicating a higher amount of EtOH is required to reach a critical point compared to IPA. This difference would be explained by the variation in steric repulsion between EtOH and IPA due to their molecular structures.[18] During exfoliation, the hydrophobic $-CH_3$ groups in EtOH and IPA face the hydrophobic surface of $Nb_2Pd_3Se_8$ (Fig. 2e), while their hydrophilic –OH groups interact with surrounding water. Thus, IPA, with more $-CH_3$ groups and a higher molecular weight, could exert a greater driving force for exfoliation and stabilization compared to EtOH.[18] To further evaluate the effect of molecular weight of the co-solvent, *tert*-butyl alcohol (TBA) was tested as a co-solvent, which

Table 1 Solvent properties used in the co-solvent exfoliation of $Nb_2Pd_3Se_8$. The surface tension and dielectric constant of NMP, previously identified as an optimal solvent, are 40.79 mJ m^{-2} and 33.0, respectively

IPA%	Surface tension (mJ m^{-2})	Dielectric constant	EtOH%	Surface tension (mJ m^{-2})	Dielectric constant
0	72.75	80.10	0	72.75	80.1
20	33.87	67.66	20	42.9	68.94
30	28.08	61.44	30	35.0	63.36
40	26.16	55.22	40	31.1	57.78
50	25.13	49.00	50	29.2	52.20
60	24.43	42.78	60	27.9	46.62
70	23.78	36.56	70	26.0	41.04
80	23.39	30.34	80	24.0	35.46
100	23.00	17.90	100	21.82	24.3

has higher molecular weight with the extra hydrophobic $-CH_3$ groups compared to EtOH and IPA (Fig. S4†). Exfoliation of $Nb_2Pd_3Se_8$ in a 50% TBA–water showed a very high exfoliation efficiency with a linear trend in the measured absorbance with respect to the molecular weights of alcohols in the co-solvent (Fig. 2f and S5†). Overall, $Nb_2Pd_3Se_8$ exhibited high dispersibility within a surface tension range of 23.4–35.0 mJ m^{-2} and a dielectric constant range of 30.3–63.4.

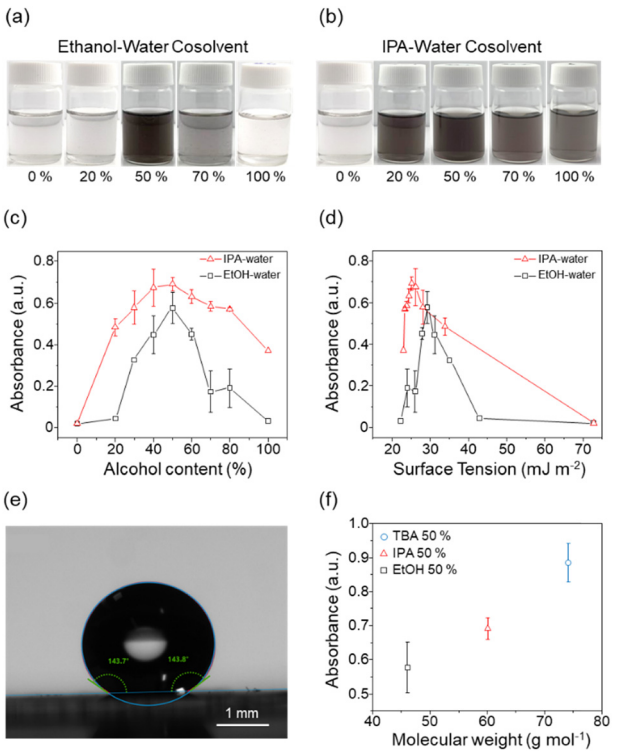

Fig. 2 Photographs of $Nb_2Pd_3Se_8$ dispersions exfoliated in (a) EtOH–water and (b) IPA–water at different volume ratios. (c) UV-vis absorbance at 400 nm depending on alcohol content. (d) UV-vis absorbance as a function of solvent surface tensions. (e) Hydrophobicity of $Nb_2Pd_3Se_8$: the contact angle of a water droplet was measured on densely packed $Nb_2Pd_3Se_8$ nanowires deposited on an AAO membrane. (f) Maximum absorbance of $Nb_2Pd_3Se_8$ exfoliated in 50% EtOH, 50% IPA and 50% TBA as a function of the molecular weights of alcohols.

We compared the efficiency of the co-solvent approach with previous LPE results in NMP. The concentrations of the dispersions obtained through the same exfoliation process was confirmed using UV-vis absorbance measurements (Fig. 3a). It was observed that both IPA–water and EtOH–water can achieve dispersion levels comparable to NMP in terms of concentration. Subsequently, three dispersions were vacuum filtered onto anodized aluminum oxide membranes to examine the morphology of the exfoliated $Nb_2Pd_3Se_8$ nanowires. The widths of $Nb_2Pd_3Se_8$ nanowires in each solvent were measured, and results were organized into a histogram (Fig. 3b). Similar to the absorbance trend, 50% IPA showed the smallest average width of 21.0 ± 5.4 nm, while 50% EtOH produced relatively thicker nanowires of 30.4 ± 7.9 nm. This can be attributed to the larger steric repulsion effect provided by greater molecular weight of IPA, promoting more sufficient exfoliation and preventing restack.[18] Fig. 3c shows the SEM images of the $Nb_2Pd_3Se_8$ nanowires exfoliated in the representative co-solvent compositions. The composition with the highest measured absorbance exhibited the smallest nanowire width (Fig. S6†). To evaluate the dispersion stability based on co-solvent compositions, the absorbance intensities of four $Nb_2Pd_3Se_8$ dispersions, processed in 50% IPA, 70% IPA, 50% EtOH and 80% EtOH, were monitored over a seven-day period (Fig. S7†). Solvents with higher exfoliation efficiency and absorbance tended to exhibit a smaller reduction in the measured absorbance after seven days. Dispersion stability appears to be significantly influenced by the size of $Nb_2Pd_3Se_8$ nanowires, which depends on exfoliation efficiency and enhances the solvation effect of solvent molecules.

Finally, FET devices using $Nb_2Pd_3Se_8$ nanowires were fabricated to evaluate the effectiveness of co-solvent exfoliation. $Nb_2Pd_3Se_8$/50% IPA dispersion was spin-coated onto a 100 nm SiO_2/Si substrate. Next, Cr/Au (5/50 nm) electrodes were deposited using standard photolithography and e-beam evaporation (Fig. 4a). We measured the transfer curve of the 13.3 nm-thick $Nb_2Pd_3Se_8$ FET, displaying n-type transport behavior as confirmed through previous studies (Fig. 4b). Its electron mobility was calculated using the following equation:

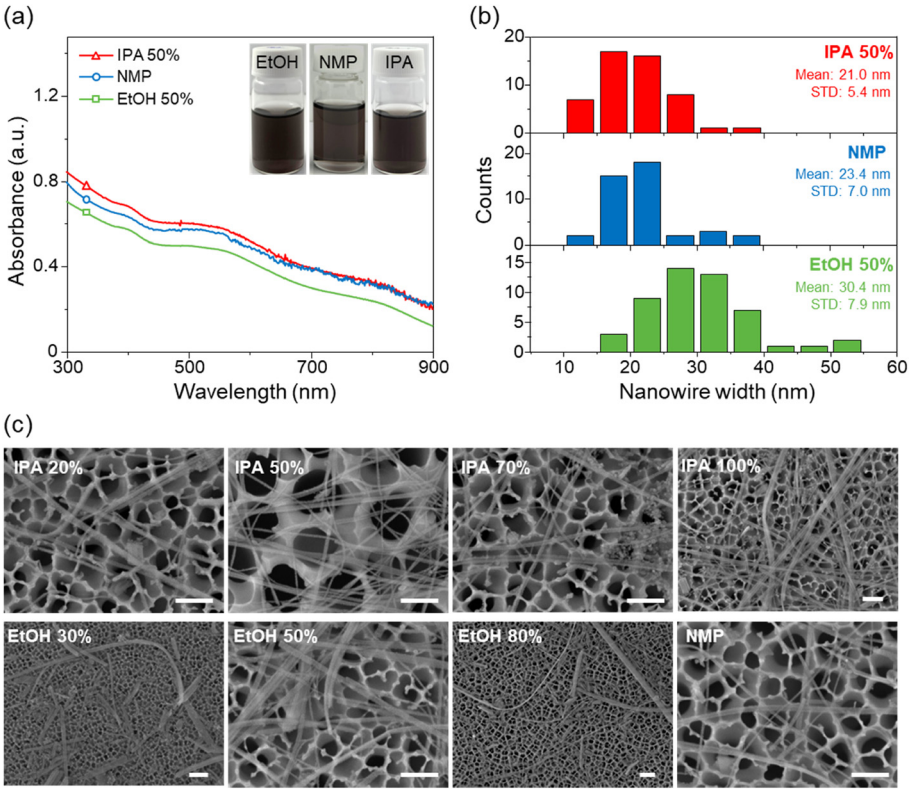

Fig. 3 (a) UV-vis spectra of $Nb_2Pd_3Se_8$ dispersions processed in 50% IPA, 50% EtOH and NMP. Inset shows photographs of the final dispersions. (b) Average width of $Nb_2Pd_3Se_8$ nanowires in different solvents. (c) SEM images of the $Nb_2Pd_3Se_8$ nanowires exfoliated in different co-solvent compositions (scale bar: 200 nm).

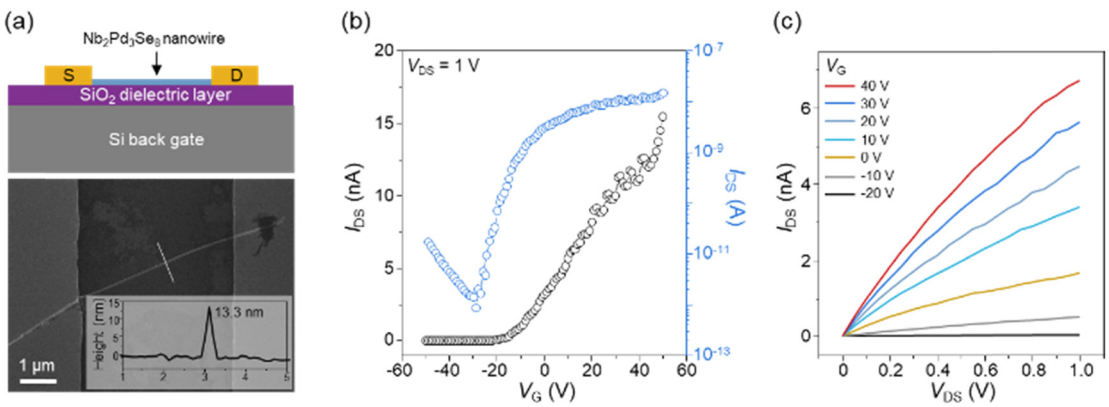

Fig. 4 (a) Device structure of the $Nb_2Pd_3Se_8$ nanowire FET (top), and the SEM image of the 13.3 nm-thick $Nb_2Pd_3Se_8$ device (bottom). (b) Transfer curve of the $Nb_2Pd_3Se_8$ FET at room temperature. (c) Output curves of the $Nb_2Pd_3Se_8$ FET.

$$\mu = (L/WC_{ox}V_{DS})(dI_{DS}/dV_G),$$

where L is the channel length, W is the channel width, and C_{ox} is the capacitance of the 100 nm SiO_2 dielectric layer per unit area. The electron mobility of the device was 10.3 cm^2 V^{-1} s^{-1}, which is comparable to that of the previous mechanically exfoliated $Nb_2Pd_3Se_8$ nanowire. Additionally, the output curves of the device showed a gradual increase in current with increasing gate bias, confirming n-type operation (Fig. 4c). In addition, FET devices were fabricated using 20% IPA and 80% EtOH dispersions to evaluate the effect of different co-solvent compositions. As previously discussed, the widths of $Nb_2Pd_3Se_8$ nanowires vary depending on the co-solvent composition. As shown in Fig. S8,† the widths of $Nb_2Pd_3Se_8$ nanowires obtained from 20% IPA, 50% IPA and 80% EtOH were 76 nm, 45 nm and 200 nm, respectively. The transfer curves of the devices displayed the highest I_{on}/I_{off} (approximately 2×10^4) and mobility observed in 50% IPA, which produced the smallest nanowire width. This size-dependent electronic properties of $Nb_2Pd_3Se_8$

nanowires have been previously demonstrated on mechanically exfoliated nanowires.[12,16] The higher I_{on}/I_{off} and mobility in thinner nanowires can be explained by the fact that the gate electric field can effectively penetrate and control the entire channel, enhancing the ability of the gate voltage to modulate the carrier concentration.[12,19] These results demonstrate that FET performance can be modulated by adjusting the co-solvent composition to produce $Nb_2Pd_3Se_8$ nanowires of varying sizes.

4. Conclusions

In conclusion, the co-solvent exfoliation of quasi-1D $Nb_2Pd_3Se_8$ nanowires was successfully demonstrated using IPA–water and EtOH–water. By testing various mixing volume ratios of the co-solvent, we identified the surface tension range in which efficient exfoliation takes place. The optimal composition of each system achieved high exfoliation efficiency, which was comparable to that of the traditional single solvent exfoliation in NMP. We believe that this approach could expand the range of applications owing to its low toxicity and low range of boiling points.

Data availability

The data that support the findings of this study are available from the corresponding author upon reasonable request.

Author contributions

K. H. Choi and Y. Kim equally contributed to this work. K. H. Choi and Y. Kim were responsible for conceptualization, investigation, methodology, and writing – original draft. J. Kang, K. I. Kim, J. S. Park, and H.-S. Oh supported the analysis and investigation. H. K. Yu and J.-Y. Choi supervised the whole project.

Conflicts of interest

There are no conflicts to declare.

Acknowledgements

This research was supported by the National Research Foundation (NRF) grant funded by the Korea government (MSIT) (No. RS-2023-00208311). In addition, this work was supported by the KIST Institutional Program (Project No. 2E31854-22-066) from the Korea Institute of Science and Technology.

References

1 J. Teeter, N. Y. Kim, T. Debnath, N. Sesing, T. Geremew, D. Wright, M. Chi, A. Z. Stieg, J. Miao and R. K. Lake, *Adv. Mater.*, 2024, 2409898.
2 D. L. M. Cordova, Y. Zhou, G. M. Milligan, L. Cheng, T. Kerr, J. Ziller, R. Wu and M. Q. Arguilla, *Adv. Mater.*, 2024, 2312597.
3 J. Klein, B. Pingault, M. Florian, M.-C. Heißenbüttel, A. Steinhoff, Z. Song, K. Torres, F. Dirnberger, J. B. Curtis and M. Weile, *ACS Nano*, 2023, **17**, 5316–5328.
4 Y. Lee, Y. W. Choi, K. Lee, C. Song, P. Ercius, M. L. Cohen, K. Kim and A. Zettl, *Adv. Mater.*, 2023, **35**, 2307942.
5 Y. Meng, W. Wang and J. C. Ho, *ACS Nano*, 2022, **16**, 13314–13322.
6 X. Liu, J. Liu, L. Y. Antipina, J. Hu, C. Yue, A. M. Sanchez, P. B. Sorokin, Z. Mao and J. Wei, *Nano Lett.*, 2016, **16**, 6188–6195.
7 X. Tan, Q. Li and D. Ren, *Phys. Chem. Chem. Phys.*, 2023, **25**, 2056–2062.
8 J.-K. Qin, P.-Y. Liao, M. Si, S. Gao, G. Qiu, J. Jian, Q. Wang, S.-Q. Zhang, S. Huang and A. Charnas, *Nat. Electron.*, 2020, **3**, 141–147.
9 J. Kim, J. Lee, J. M. Lee, A. Facchetti, T. J. Marks and S. K. Park, *Small Methods*, 2024, **8**, 2300246.
10 Y. Ma, H. Yi, H. Liang, W. Wang, Z. Zheng, J. Yao and G. Yang, *Mater. Futures*, 2024, **3**, 012301.
11 L. Du, Y. Zhao, L. Wu, X. Hu, L. Yao, Y. Wang, X. Bai, Y. Dai, J. Qiao and M. G. Uddin, *Nat. Commun.*, 2021, **12**, 4822.
12 B. J. Jeong, K. H. Choi, J. Jeon, S. O. Yoon, Y. K. Chung, D. Sung, S. Chae, B. J. Kim, S. Oh and S. H. Lee, *Adv. Funct. Mater.*, 2022, **32**, 2108104.
13 B. J. Jeong, B. Lee, K. H. Choi, D. Sung, S. Ghods, J. Lee, J. Jeon, S. Cho, S. H. Lee and B. J. Kim, *Nano Lett.*, 2023, **23**, 6269–6275.
14 S. H. Lee, B. J. Jeong, K. H. Choi, J. Jeon, B. Lee, S. Cho, D. Kim, G. T. Gudena, D. D. Megersa and S. H. Kim, *CrystEngComm*, 2024, **26**, 4541–4550.
15 Q. Qin, W. Gao, H. Zhang, J. Chen, Y. Yan, K. Zhu, M. Long, G. Li, S. Yin and Y. Du, *J. Mater. Chem. A*, 2023, **11**, 11517–11525.
16 K. H. Choi, J. Jeon, B. J. Jeong, S. Chae, S. Oh, C. Woo, T. Y. Kim, J. Ahn, J. H. Lee and H. K. Yu, *Adv. Mater. Interfaces*, 2022, **9**, 2200620.
17 J. Shen, J. Wu, M. Wang, P. Dong, J. Xu, X. Li, X. Zhang, J. Yuan, X. Wang and M. Ye, *Small*, 2016, **12**, 2741–2749.
18 U. Halim, C. R. Zheng, Y. Chen, Z. Lin, S. Jiang, R. Cheng, Y. Huang and X. Duan, *Nat. Commun.*, 2013, **4**, 2213.
19 Y. Sui and J. Appenzeller, *Nano Lett.*, 2009, **9**, 2973–2977.

